ACS APPLIED MATERIALS & INTERFACES

ACS AUTHORCHOICE

www.acsami.org

Research Article

Synthesis and Characterization of Polypyrrole-Coated Anthracene Microparticles: A New Synthetic Mimic for Polyaromatic Hydrocarbon-Based Cosmic Dust

Derek H. Chan, Arthur Millet, Callum R. Fisher, Mark C. Price, Mark J. Burchell, and Steven P. Armes*

Cite This: *ACS Appl. Mater. Interfaces* 2021, 13, 3175–3185

Read Online

ACCESS | Metrics & More | Article Recommendations | Supporting Information

ABSTRACT: Polyaromatic hydrocarbons (PAHs) are found throughout the universe. The ubiquity of these organic molecules means that they are of considerable interest in the context of cosmic dust, which typically travels at hypervelocities (>1 km s^{-1}) within our solar system. However, studying such fast-moving micrometer-sized particles in laboratory-based experiments requires suitable synthetic mimics. Herein, we use ball-milling to produce microparticles of anthracene, which is the simplest member of the PAH family. Size control can be achieved by varying the milling time in the presence of a suitable anionic commercial polymeric dispersant (Morwet D-425). These anthracene microparticles are then coated with a thin overlayer of polypyrrole (PPy), which is an air-stable organic conducting polymer. The uncoated and PPy-coated anthracene microparticles are characterized in terms of their particle size, surface morphology, and chemical structure using optical microscopy, scanning electron microscopy, laser diffraction, aqueous electrophoresis, FT-IR spectroscopy, Raman microscopy, and X-ray photoelectron spectroscopy (XPS). Moreover, such microparticles can be accelerated up to hypervelocities using a light gas gun. Finally, studies of impact craters indicate carbon debris, so they are expected to serve as the first synthetic mimic for PAH-based cosmic dust.

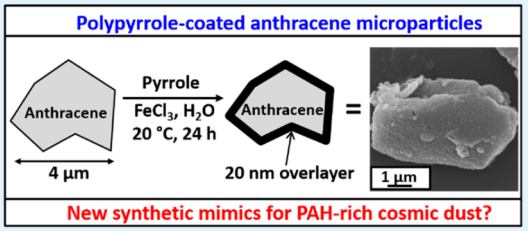

KEYWORDS: *cosmic dust, anthracene, polyaromatic hydrocarbons, polypyrrole, conducting polymers, hypervelocity impacts, microparticles, space science*

INTRODUCTION

Polyaromatic hydrocarbons (PAHs) such as anthracene, phenanthrene, perylene, and pyrene are naturally occurring molecules found in coal and petroleum deposits, oil shale, hydrothermal vents, and volcanic ash.[1] They are also present in cigarette smoke and automotive exhaust gas and can be generated during wood burning. As such, PAHs are considered to be long-lived organic pollutants whose persistence in the environment is linked to their strong resistance to oxidative and photochemical degradation. However, it is this chemical stability that has attracted growing interest from the space science community, not least because infrared emission spectroscopy studies have confirmed the ubiquitous presence of PAHs throughout the universe.[2−5] Indeed, Greenberg et al. have postulated that photoprocessing of organic dust mantles within the interstellar medium during solar irradiation may be a possible mechanism for generating PAHs.[6] More recently, PAHs have been detected in Martian meteorites,[7] in interplanetary dust,[2,8] in the upper atmosphere of Titan,[9,10] and within comets.[11,12] They have even been implicated as an important component in the emergence of early life on Earth—the so-called "Aromatic World" hypothesis.[13,14] Moreover, one of the objectives of the ExoMars rover mission is to search for such molecules up to 2 m below the surface of the Martian soil.[15]

In principle, laboratory-based high-energy impact experiments can shed considerable light on the behavior of various types of micrometeorites, which typically travel at hypervelocities (>1 km s^{-1}) in outer space.[16] This is because when such fast-moving micrometeorites strike a metal target, they are almost instantaneously converted into molecular and/or atomic fragments by the high-energy impact.[17] This enables their chemical composition to be inferred by time-of-flight mass spectrometric analysis of the ionic plasma.[18−21] Indeed, this was the fundamental detection mechanism for the Cosmic Dust Analyzer (CDA) instrument deployed by the CASSINI spacecraft when orbiting Saturn and its moons.[22] For example, this CDA detector has detected both low- and high-mass aromatic compounds within the plumes of water ejected from the interior of the Saturnian satellite Enceladus.[23,24]

In practice, it is not trivial to design appropriate synthetic mimics that can be accelerated up to the hypervelocity regime

Received: November 4, 2020
Accepted: December 24, 2020
Published: January 6, 2021

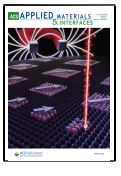

https://dx.doi.org/10.1021/acsami.0c19758
ACS Appl. Mater. Interfaces 2021, 13, 3175–3185

that typically characterizes the behavior of such "cosmic dust". Nevertheless, Armes and co-workers have prepared a series of (sub)micrometer-sized particles that have proven to be useful mimics for either carbonaceous- or silicate-rich micrometeorites.[16] This has been achieved by coating either polystyrene or silica particles with an ultrathin overlayer of polypyrrole (PPy).[25,26] This relatively air-stable organic conducting polymer ensures that such synthetic particles can acquire sufficient surface charge to enable their electrostatic acceleration up to the hypervelocity regime using a high-field van de Graaff accelerator.[27] In addition, certain naturally occurring mineral grains such as olivine, pyroxene, and pyrrhotite have been coated with PPy and successfully accelerated for hypervelocity impact experiments.[28−30] Moreover, by coating appropriate latex particles with PPy,[31] it has been possible to demonstrate via laboratory experiments that impact ionization time-of-flight spectra can be used to distinguish between at least some types of aromatic and aliphatic organic microparticles.[20,32] However, it has not yet been possible to examine PAH-based particles in this context. One of the simplest members of the PAH family is anthracene (see Figure 1). This

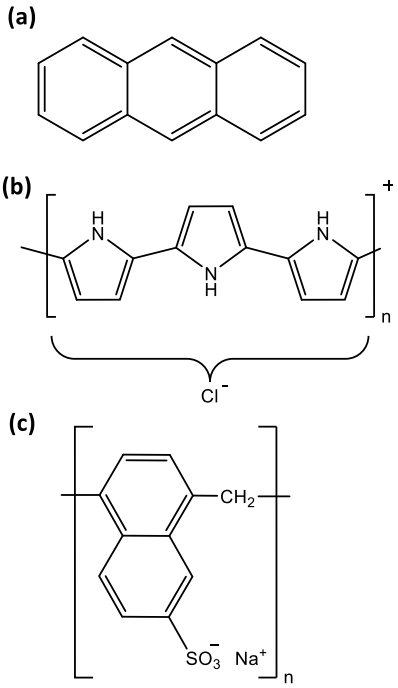

Figure 1. Chemical structures for (a) anthracene, (b) polypyrrole (PPy), and (c) Morwet D-425 dispersant. [N.B. The chemical structure shown for PPy is the typical idealized structure reported in the literature; in reality, the conjugated backbone also contains unpaired electrons (radicals) as well as delocalized cationic charge].

planar fused molecule forms large organic crystals with very limited solubility in common organic solvents and is essentially insoluble in water. Herein, we report the convenient preparation of micrometer-sized anthracene particles via ball-milling in the presence of a commercial dispersant (Morwet D-425) and demonstrate that the controlled deposition of PPy from aqueous solution can be used to coat such microparticles with good precision. These new microparticles are expected to become useful synthetic PAH mimics for laboratory-based hypervelocity experiments using either a light gas gun[27,33,34] or a van de Graaff accelerator.[17,33]

EXPERIMENTAL SECTION

Materials. Iron(III) chloride hexahydrate (97%) was purchased from Alfa Aesar (UK). $(NH_4)_2S_2O_8$ (APS), anthracene (97%), and pyrrole were each purchased from Sigma-Aldrich (UK). Pyrrole was purified by alumina chromatography (basic alumina, Sigma-Aldrich UK) prior to use. Silicone SAG1572 (Momentive, Germany) was used as an antifoaming agent, while Morwet D-425 (Nouryon, Sweden; molecular weight range = 1 000 to 5 000 g mol^{-1}) was used as a dispersant. Deionized water was obtained from an Elga Medica DV25 water purification unit. Finally, 1.0 mm ceramic beads (zirconium aluminum oxide) were obtained from Sigmund-Lindner (Germany).

Synthesis of PPy Bulk Powder. $FeCl_3{\cdot}6H_2O$ (9.10 g) was dissolved in deionized water (100 mL) in a 125 mL glass bottle, and this orange-brown aqueous solution was stirred using a magnetic stirrer bar. The pyrrole monomer (1.0 mL) was added to this reaction solution and allowed to polymerize for 12 h at 20 °C. The resulting black precipitate was vacuum-filtered using a Buchner funnel and washed first with deionized water and then methanol. The purified moist black powder was placed on a petri dish and dried in a 50 °C oven overnight. The approximate isolated yield of PPy was 0.87 g (73% based on the pyrrole monomer).

Preparation of Anthracene Microparticles. *(a) By IKA Ultra-Turrax tube drive.* Anthracene (2.28 g, 20% w/w), Morwet D-425 dispersant (0.2850 g, 2.5% w/w), silicone antifoam (0.114 g, 1.0% w/w), and deionized water (8.72 g, 76.5% w/w) were mixed in a 30 mL tube with approximately 15 g of 1 mm ceramic beads. The tube was then attached to the IKA Ultra-Turrax tube drive and milled at 6 000 rpm for 90 to 120 min until the target particle size was achieved. The ceramic beads were then removed by filtration to obtain a white free-flowing aqueous dispersion.

(b) By Retsch Planetary Ball Mill. Anthracene (5.00 g, 20% w/w), Morwet D-425 (0.6250 g, 2.5% w/w) dispersant, silicon antifoam (0.250 g, 1.0% w/w), and deionized water (19.125 g, 76.5% w/w) were added to a 50 mL ball-milling jar together with 10 g of 2 mm beads. This mixture was milled at 250 rpm using a Retsch Planetary Ball Mill PM 100 for a rotation time of 15 min and a break time of 10 min at 250 rpm. Once the target particle size was achieved, the ceramic beads were removed by filtration to obtain a white free-flowing dispersion.

Purification of Aqueous Anthracene Dispersions to Remove Excess Dispersant. Aqueous anthracene dispersions were subjected to three centrifugation−redispersion cycles (6 000 rpm, 10 min per cycle). Each cycle required careful decantation of the aqueous supernatant and redispersion of the sediment using fresh deionized water. The purified aqueous dispersions were either then freeze-dried to recover anthracene microparticles in the form of a fine white powder or coated with an ultrathin overlayer of PPy prior to further characterization studies.

Synthesis of PPy-Coated Anthracene Crystals. The following protocol was used to coat 0.50 g of 4 μm anthracene microparticles with a target PPy overlayer of 20 nm and is representative. A 20% w/w aqueous dispersion of anthracene microparticles (2.50 g), pyrrole (37.0 μL; equivalent to a mass loading of 3.5%), and deionized water (25.0 mL) were added to a 120 mL glass bottle to give a low-viscosity dispersion. $FeCl_3{\cdot}6H_2O$ (0.34 g) was dissolved in deionized water (5.0 mL), and the final aqueous dispersion was stirred for 24 h at 20 °C. The resulting black dispersion was purified by three centrifugation−dispersion cycles (6 000 rpm, 10 min) to remove excess inorganic salts and any unreacted pyrrole and then freeze-dried overnight to recover a fine black powder. To target other PPy overlayer thicknesses, the masses of anthracene and water were kept constant and the amounts of the pyrrole monomer and $FeCl_3$ oxidant were varied accordingly (always employing a fixed oxidant/monomer molar ratio of 2.33).

Table 1 summarizes the various target and actual PPy mass loadings required to achieve a desired nominal overlayer thickness. Such mass loadings depend on the mean diameter of the anthracene microparticles and the solid-state densities of the anthracene (1.25 g cm^{-3}) and PPy (1.46 g cm^{-3}), which were determined by helium

https://dx.doi.org/10.1021/acsami.0c19758
ACS Appl. Mater. Interfaces 2021, 13, 3175−3185

Table 1. Summary of the Target PPy Overlayer Thicknesses, Target PPy Mass Loadings, Nitrogen Microanalyses, and Actual PPy Mass Loadings (Calculated by Nitrogen Microanalyses) for the Two Types of Anthracene Microparticles Prepared in this Study

sample description	anthracene microparticle diameter[a] (μm)	target PPy overlayer thickness (nm)	target PPy mass loading (%)	nitrogen microanalysis[b] (%)	Calculated PPY mass loading from nitrogen microanalysis (%)
PPy bulk powder	N/A	N/A	N/A	15.90	N/A
uncoated anthracene	4	N/A	N/A	0.0	N/A
PPy-coated anthracene	4	10	1.8	0.0	0.0
PPy-coated anthracene	4	20	3.5	0.43	2.7 ± 1.9
PPy-coated anthracene	4	30	5.0	0.96	6.0 ± 1.9
PPy-coated anthracene	2	20	6.7	1.36	8.6 ± 1.9

[a]As determined by laser diffraction studies. [b]Nitrogen microanalysis has an error of ± 0.30%.

pycnometry. Similar calculations have been previously reported by Lascelles and Armes, who assumed a core−shell morphology to derive a simple equation for coating experiments involving well-defined spherical polystyrene latex particles (see Supporting Information).[25]

In the present case, the core comprises anthracene, while the shell is composed of PPy. In practice, the anthracene microparticles do not have a well-defined spherical morphology (see later). Thus, the target PPy overlayer thicknesses are calculated for "sphere-equivalent" anthracene microparticles. It is implicitly assumed that (i) all of the pyrrole is converted into PPy and (ii) all of the PPy is deposited onto the surface of the anthracene microparticles. In principle, the actual PPy mass loading can be calculated by nitrogen microanalysis by comparing the nitrogen content of the PPy-coated anthracene microparticles to that of PPy bulk powder prepared in the absence of any anthracene microparticles.[25]

Characterization Techniques. *Helium Pycnometry.* The solid-state densities of anthracene and PPy bulk powder were determined to be 1.25 and 1.46 g cm^{-3}, respectively, using a Micromeritics AccuPyc 1330 instrument operating at 20 °C.

Optical Microscopy. Optical images were recorded using a Cole−Palmer compound optical microscope equipped with a LCD tablet display and a Moticam BTW digital camera. This technique was used to estimate the mean number−average diameter of the anthracene microparticles (approximately 100 particles counted per sample).

Particle Size Analysis by Laser Diffraction. Uncoated and PPy-coated anthracene microparticles were analyzed using a Malvern Mastersizer 3000 laser diffraction instrument equipped with a Hydro EV sample dispersion unit, a He−Ne laser (λ = 633 nm), and a solid-state blue laser (λ = 466 nm). The stirring rate was set at 2000 rpm, and data from five measurements were averaged. The standard operating procedure parameters were asssumed non-spherical particles with an absorption index of 0.01. The refractive index for anthracene was taken to be 1.5948 (see http://www.chemspider.com/Chemical-Structure.8111.html).

Solution Densitometry. The solution densities of a series of aqueous solutions of Morwet D-425 (ranging from 0.05 to 3.00% w/w) were determined using an Anton Paar DMA 4500 M density meter at 20 °C. Subsequently, ball-milled anthracene dispersions with mean diameters of either 2 or 4 μm were centrifuged at 10 000 rpm for 10 min and the solution densities of their respective supernatants were measured. This information was used to calculate the amount of Morwet D-425 that was adsorbed onto the surface of the anthracene microparticles.

Scanning Electron Microscopy. Images were obtained using an Inspect-F instrument operating at an accelerating voltage of 5 kV. Each powder was dispersed and dried onto a thin glass layer before being sputter-coated with a 5 nm overlayer of gold to prevent sample charging.

FT-IR Spectroscopy. FT-IR spectra were recorded for the uncoated anthracene microparticles, PPy bulk powder, and PPy-coated anthracene microparticles using a Thermo Scientific Nicolet iS10 spectrometer equipped with a Diamond ATR Golden Gate accessory. The spectral resolution was 4 cm^{-1} and 32 scans were averaged per spectrum.

Raman Microscopy. Raman spectra were recorded using a HORIBA LabRam-HR spectrometer equipped with an infrared laser (λ = 785 nm, 3 mW). This wavelength was selected to minimize the well-known problem of fluorescence associated with the Raman spectra of polymers.[36] Given the well-known strongly absorbing nature of highly conjugated polymers such as PPy,[37] either 1 or 10% filters were employed to attenuate the laser power in order to avoid sample degradation. The spectrometer utilized a 600 mm^{-1} grating with a spectral resolution of approximately 2 cm^{-1} and an Olympus BX41 microscope equipped with a ×100 objective lens, which provided a spatial resolution of 1−2 μm. The spectra were obtained from individual anthracene microparticles, with typically five spectra being averaged per sample.

Aqueous Electrophoresis. Zeta potential versus pH curves were constructed using a Malvern Zetasizer NanoZS instrument operating at 20 °C. Measurements were conducted on dilute (0.5% w/w) aqueous dispersions in the presence of 1 mM KCl as the background electrolyte, with the pH being adjusted using either NaOH or HCl. Zeta potentials were calculated from an average of three measurements via the Henry equation using the Smoluchkowski approximation.

X-ray Photoelectron Spectroscopy. Uncoated and PPy-coated anthracene microparticles and PPy bulk powder were analyzed in turn by X-ray photoelectron spectroscopy (XPS) using a Kratos Axis Supra X-ray photoelectron spectrometer. Step sizes of 0.5 and 0.05 eV were used to record the survey spectra and high resolution coreline spectra, respectively. In each case, powders were placed on an indium foil and spectra were recorded from at least two separate areas.

Light Gas Gun Experiments and Impact Crater Analysis. A two-stage light gas gun[27] was used to fire PPy-coated anthracene microparticles (4 μm diameter; coated with a nominal PPy overlayer thickness of 30 nm) at an aluminum foil target with a mean thickness of 110 μm. The target chamber was evacuated to less than 0.5 mbar while firing the gun, and the shot speed was determined to be 1.87 km s^{-1} (±0.5%). After this shot, the aluminum foil target was examined using a Hitachi S4700-N FEG-SEM instrument equipped with a Bruker Xflash EDX detector to identify impact craters caused by the impinging microparticles.

RESULTS AND DISCUSSION

It is well known that ball-milling can be used to prepare micron-sized particles of molecular organic crystals. For example, this technology is widely used to prepare aqueous suspensions of agrochemical actives.[38,39] We envisaged that the same approach should be applicable to PAHs such as

https://dx.doi.org/10.1021/acsami.0c19758
ACS Appl. Mater. Interfaces 2021, 13, 3175−3185

anthracene, which form relatively large crystals. Accordingly, ball milling was used to prepare aqueous dispersions of anthracene microparticles using a commercially available anionic polymeric dispersant (Morwet D-425) to prevent aggregation of the microparticles via a steric stabilization mechanism.[40,41] Two commercial ball-milling devices were examined: an IKA Ultra-Turrax tube drive was used to ball-mill relatively small quantities of material, while a planetary ball mill enabled larger (multigram) quantities to be processed. A substantial reduction in the mean size of the anthracene microparticles was achieved in both cases. Figure 2a shows the

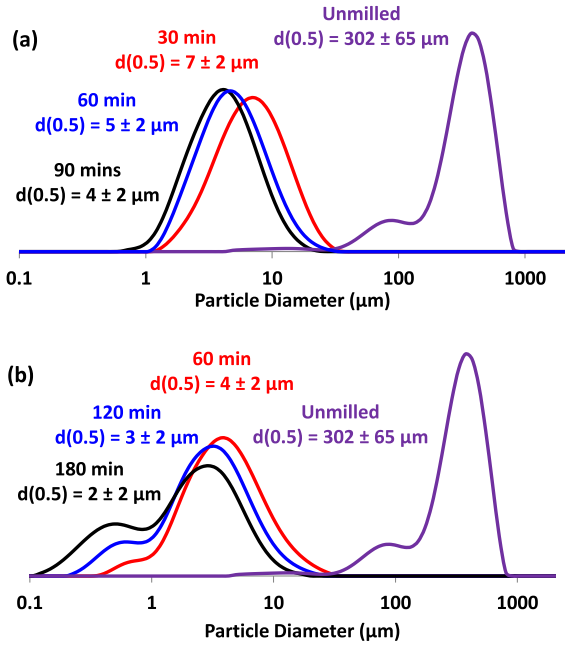

Figure 2. Laser diffraction particle size distribution curves obtained for the reduction in anthracene particle size via ball milling in the presence of Morwet D-425 dispersant using (a) the IKA Ultra-Turrax tube drive and (b) retsch planetary ball mill.

laser diffraction size distributions obtained for the initial anthracene crystals and the anthracene microparticles obtained after grinding an aqueous suspension of anthracene for 30−90 min in the presence of Morwet D-425 dispersant using the tube drive. This particle sizing technique reports a "sphere-equivalent" volume−average diameter, $d(0.5)$, which is defined such that 50% of the particles fall below this size. The as-supplied anthracene crystals have an initial volume−average diameter of 302 ± 65 μm, but this was reduced to 7 ± 2 μm within a milling time of 30 min. Longer milling times (60−90 min) produced reasonably uniform microparticles with a volume−average diameter of 4 ± 2 μm, but thereafter, there was little or no further reduction in mean particle size.

Even smaller microparticles could be achieved using the planetary ball mill (see Figures 2b and S1). However, the latter technique usually gave broader size distributions owing to the formation of a population of relatively fine particles. It is noteworthy that mean anthracene microparticle diameters of 2−4 μm are comparable with that expected for PAH-based microparticles in space. For example, the NASA *Stardust* mission collected similar-sized cometary dust within its aerogel targets during a cometary fly-by at 6.1 km s^{-1}[42,43] Moreover, the plumes of water erupting from the interior of the Jovian satellite Europa and the Saturnian satellite Enceladus are also believed to contain microparticles within this size range.[44,45]

The aqueous dispersion of anthracene microparticles was purified to remove excess non-adsorbed dispersants. This was achieved by three centrifugation−redispersion cycles, with careful decantation of each supernatant prior to redispersion of the sedimented microparticles. Laser diffraction studies indicated no change in the mean anthracene particle size after washing, suggesting a colloidally stable dispersion (Figure S2). Solution densitometry was used to monitor the concentration of the Morwet D-425 dispersant in the aqueous phase before and after ball-milling (see Figure S3). These measurements indicated that the 4 μm anthracene microparticles contained approximately 0.50% Morwet D-425 by mass. As expected, the 2 μm anthracene microparticles contained a higher Morwet D-425 content (1.50% by mass).

PPy is readily prepared in aqueous solution using mild chemical oxidants such as $FeCl_3$. It is usually obtained in the form of an insoluble macroscopic precipitate that has a distinctive globular morphology (see Figure S4), but it is well known that PPy can be deposited onto various types of colloidal particles with good control over its coating thickness.[25,37,46] This aqueous deposition process works rather well for hydrophobic substrates such as polystyrene latex but is less suitable for hydrophilic substrates such as silica, for which chemical modification of the surface is usually required.[25,47−49] However, for the highly hydrophobic anthracene microparticles reported herein, the aqueous deposition of PPy was expected to be straightforward.

Accordingly, the pyrrole monomer and $FeCl_3{\cdot}6H_2O$ oxidant were added to an aqueous dispersion of anthracene microparticles, and the pyrrole polymerization was allowed to proceed for 24 h at 20 °C. The PPy-coated anthracene microparticles were then subjected to three centrifugation−redispersion cycles to remove the spent oxidant and any unreacted pyrrole prior to freeze-drying overnight (Figure 3). Some of this purified aqueous dispersion was retained for particle size analysis.

The mean particle size of the purified PPy-coated anthracene microparticles was assessed using laser diffraction (Figure 4).

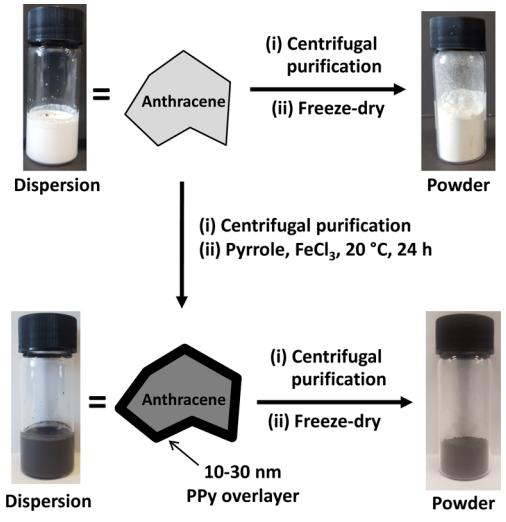

Figure 3. Schematic representation of the aqueous deposition of an ultrathin PPy overlayer onto the surface of ball-milled Morwet-stabilized anthracene microparticles.

https://dx.doi.org/10.1021/acsami.0c19758
ACS Appl. Mater. Interfaces 2021, 13, 3175−3185

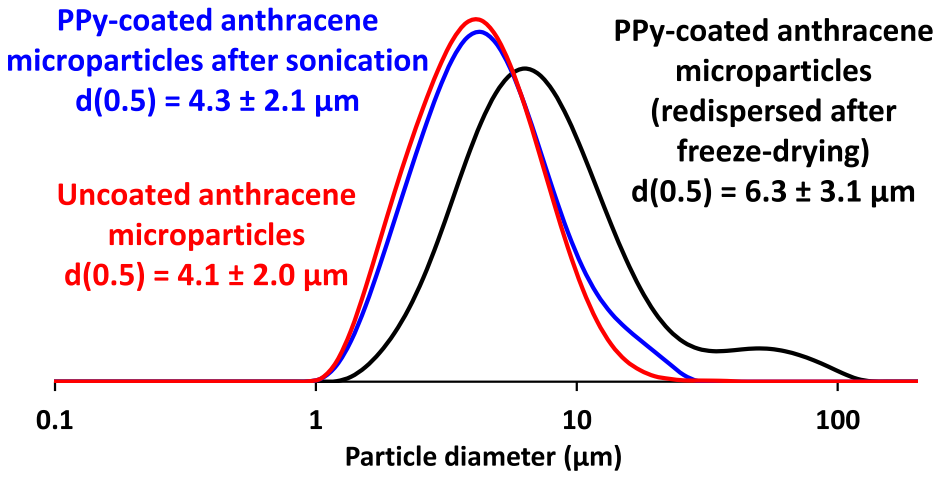

Figure 4. Laser diffraction particle size distribution curves recorded for an aqueous suspension of uncoated anthracene microparticles (red) and PPy-coated anthracene microparticles before (black) and after (blue) ultrasonication.

The dried black powder proved to be relatively hydrophobic, so a wetting agent, Aerosol OT-B (0.01% w/w based on PPy-coated anthracene microparticles), was required to disperse it. A volume−average diameter of approximately 6 ± 3 μm was determined, which was significantly larger than what was expected, given that a PPy overlayer of just 20 nm was targeted. This indicates incipient flocculation of the PPy-coated anthracene microparticles during drying, which is not unexpected in view of the relatively high Hamaker constant for this conducting polymer.[50] However, ultrasonication for 3 min just prior to laser diffraction analysis enables the microparticle floccs to be broken up. This protocol produces a volume−average diameter of 4.3 ± 2.1 μm, which is comparable to that of the original uncoated Morwet-stabilized anthracene microparticles (Figure 4).

Optical microscopy images of the milled anthracene microparticles obtained using Morwet D-425 were in good agreement with the laser diffraction measurements (Figure 5a,c). The visual appearance of the PPy-coated anthracene microparticles did not differ significantly from that of the uncoated anthracene microparticles (Figure 5b,d). This is attributed to the rather low conducting polymer mass loadings and hence relatively thin overlayers (Table 1). It is perhaps worth emphasizing that the PPy grain size is around 5−10 nm,[51] so a PPy thickness of 10 nm is essentially the thinnest coating that can be targeted to achieve a contiguous overlayer, which is required for the efficient accumulation of surface charge in van de Graaff accelerator experiments.[16−21]

Scanning electron microscopy (SEM) studies indicate that the milled anthracene microparticles were somewhat ill-defined in terms of their size and morphology (Figure 6a,b). Nevertheless, the mean microparticle dimensions are consistent with those indicated by optical microscopy and laser diffraction studies. There is also some evidence for an unusual perforated, porous surface morphology. Targeting a PPy loading of 3.5% by mass (mean coating thickness = 20 nm) produced a relatively uniform overlayer (Figure 6c). The

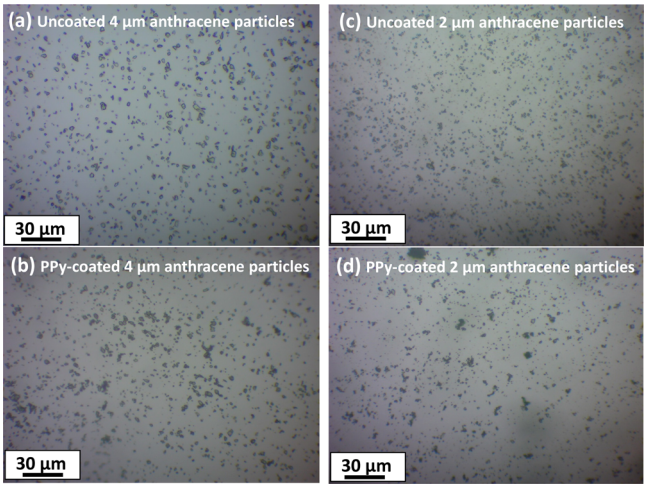

Figure 5. Optical microscopy images recorded for (a) uncoated and (b) PPy-coated 4 μm anthracene microparticles (PPy overlayer thickness = 20 nm) and (c) uncoated and (d) PPy-coated 2 μm anthracene microparticles (PPy overlayer thickness = 20 nm).

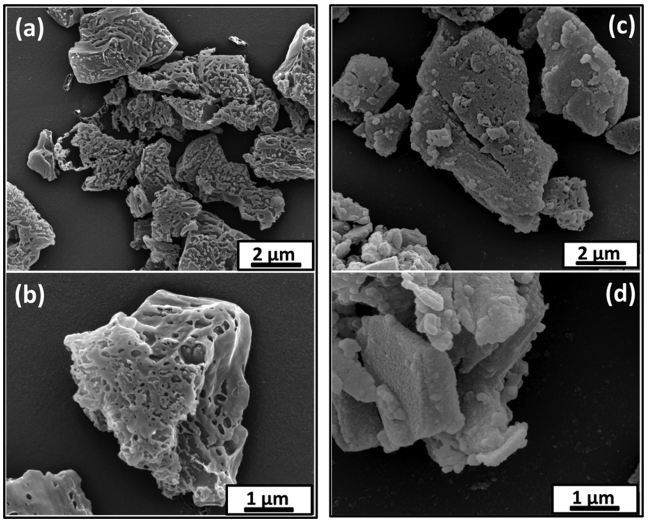

Figure 6. SEM images recorded for (a,b) uncoated 4 μm anthracene microparticles and (c,d) PPy-coated 4 μm anthracene microparticles (PPy mass loading = 3.5%, corresponding to a mean coating thickness of 20 nm).

https://dx.doi.org/10.1021/acsami.0c19758
ACS Appl. Mater. Interfaces 2021, 13, 3175−3185

deposited PPy overlayer has a distinct globular morphology that resembles that of PPy bulk powder (see Figure S4 in the Supporting Information), albeit with finer features. The same PPy morphology was observed on smaller 2 μm anthracene microparticles, which were coated with a target overlayer of 20 nm (Figure S1). A similar surface morphology has been observed for other PPy-coated particles.[37] Moreover, the surface voids observed for the uncoated anthracene microparticles were no longer visible for the PPy-coated anthracene microparticles (Figure 6d).

The nitrogen content of PPy bulk powder is 15.9% by mass (see Table 1). However, the highest target PPy mass loading for the anthracene microparticles (which have zero nitrogen content) was 6.7%, which means that their nitrogen contents should be of the order of 1.0% by mass. Given that the generally accepted accuracy for nitrogen microanalysis is typically ±0.30%, this technique is clearly not very reliable for compositional analysis of this particular system. Nevertheless, we conducted nitrogen microanalyses of PPy bulk powder and the four examples of PPy-coated anthracene microparticles (see Table 1). Within the admittedly large experimental uncertainty, the PPy mass loadings calculated from the nitrogen microanalyses are consistent with those targeted, with higher PPy loadings being obtained when coating finer anthracene microparticles (2 vs 4 μm diameter).

Transmission mode FT-IR spectra recorded for PPy bulk powder, milled anthracene microparticles prepared using the Morwet D-425 dispersant, and a series of PPy-coated anthracene microparticles are shown in Figure 7. The latter three samples exhibit strong bands at 1550, 1180, and 1030 cm^{-1}, corresponding to the PPy overlayer, which became more intense as thicker PPy overlayers are targeted.

Raman spectra recorded for PPy bulk powder, pure anthracene, and PPy-coated anthracene microparticles are shown in Figure 8. The Raman spectrum for pure anthracene exhibited strong sharp bands at 121, 395, 752, 1401, and 1556 cm^{-1}, which correspond well to those reported in the literature.[52] The PPy bulk powder reference spectrum

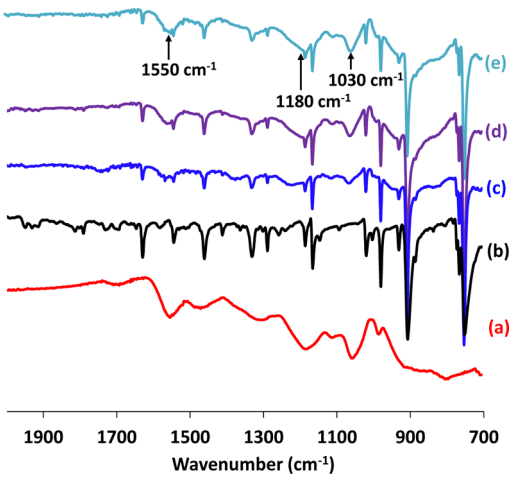

Figure 7. FT-IR spectra recorded for (a) PPy bulk powder; (b) uncoated milled 4 μm anthracene microparticles prepared using the Morwet D-425 dispersant; (c) 4 μm anthracene microparticles coated with a nominal 10 nm PPy overlayer; (d) 4 μm anthracene microparticles coated with a nominal 20 nm PPy overlayer; and (e) 4 μm anthracene microparticles coated with a nominal 30 nm PPy overlayer.

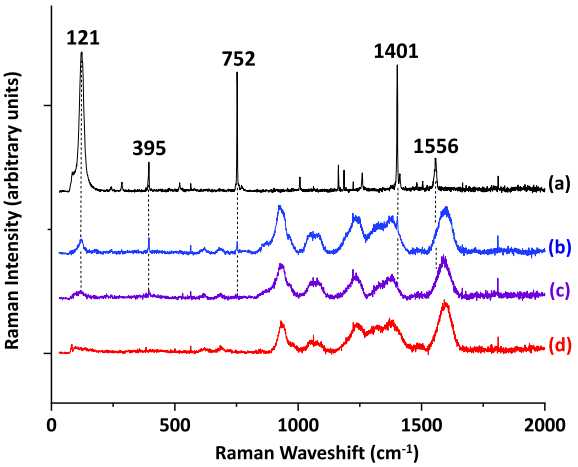

Figure 8. Raman spectra recorded for (a) pure anthracene crystals, (b) PPy-coated 4 μm anthracene microparticles (target PPy overlayer thickness = 10 nm), (c) PPy-coated 4 μm anthracene microparticles (target PPy overlayer thickness = 20 nm), and (d) PPy bulk powder. The five most intense Raman lines in the pure anthracene crystals are at 121, 395, 752, 1401, and 1556 cm^{-1} (see vertical dashed lines), which is in good agreement with the literature.[52] The two spectra obtained for the PPy-coated anthracene microparticles are both dominated by signals from the conducting polymer component owing to a resonance Raman effect.

exhibited strong broad bands at 925, 1066, 1237, 1370, and 1592 cm^{-1}, which are in good agreement with our previously reported observations.[47−51]

The Raman spectrum recorded for the anthracene microparticles coated with a nominal 10 nm PPy overlayer is strikingly similar to that recorded for the PPy bulk powder, with relatively weak bands attributable to the underlying anthracene being observed at 121, 395, 752, and 1401 cm^{-1}.[53−57] There is also some evidence for the 1592 cm^{-1} band as a rather weak shoulder on a strong PPy band. The first four bands are also present for the anthracene microparticles coated with a nominal 20 nm PPy overlayer, although they are all somewhat attenuated (compare Figure 8b,c). These observations are rather remarkable, given that the 10 nm PPy-coated anthracene microparticles contain more than 98% anthracene by mass (see Table 1). Similar observations have been previously reported for PPy-coated latex particles and have been explained in terms of a resonance Raman effect. This leads to efficient absorption of the incident laser light by the conducting polymer overlayer, which causes obscuration of the underlying substrate.[30,41,51] It is perhaps worth emphasizing that such attenuation is much weaker for infrared radiation (see Figure 7). In summary, these observations provide good evidence for a relatively uniform, rather than patchy, PPy overlayer at the surface of the anthracene microparticles. Such a core−shell morphology is highly desirable if such synthetic mimics are to be useful in the context of space science applications. For light gas gun experiments, it means that the PPy overlayer can serve as a sacrificial layer with a strong spectroscopic signature, which makes such microparticles potentially useful when assessing the likely extent of thermal ablation suffered by PAH dust grains during their capture within aerogel targets at hypervelocities of 1−6 km s^{-1}.[33] Similarly, a contiguous PPy overlayer should enable the efficient accumulation of surface charge, which is a prerequisite

https://dx.doi.org/10.1021/acsami.0c19758
ACS Appl. Mater. Interfaces 2021, 13, 3175−3185

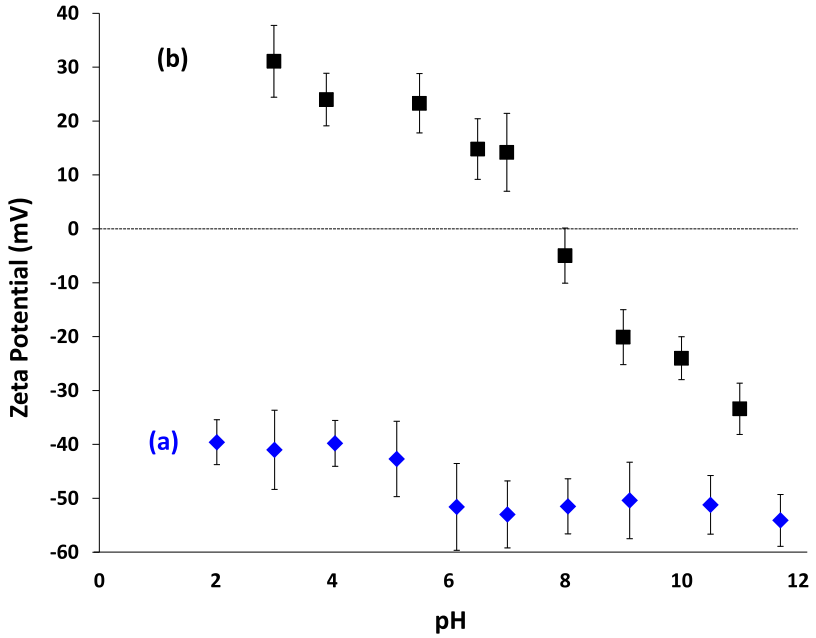

Figure 9. Zeta potential versus pH curves recorded for (a) 4 μm anthracene microparticles prepared using the anionic Morwet D-425 dispersant and (b) PPy-coated 4 μm anthracene microparticles (nominal overlayer thickness = 20 nm).

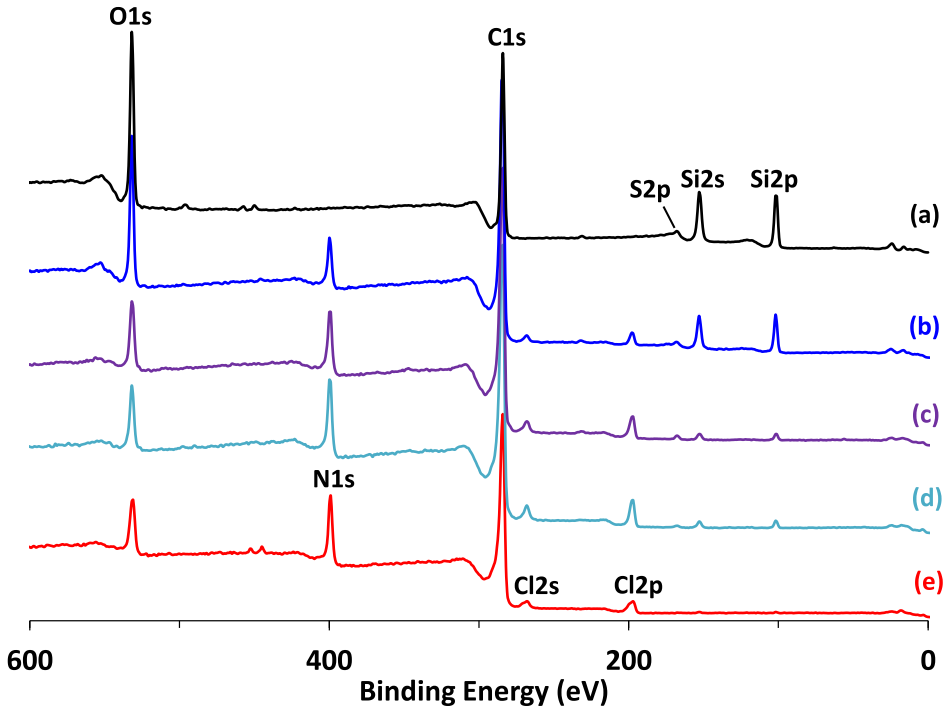

Figure 10. X-ray photoelectron survey spectra recorded for (a) uncoated milled 4 μm anthracene microparticles prepared using the Morwet D-425 dispersant; (b) PPy-coated 4 μm anthracene microparticles (nominal overlayer thickness = 10 nm); (c) PPy-coated 4 μm anthracene microparticles (nominal overlayer thickness = 20 nm); (d) PPy-coated 4 μm anthracene microparticles (nominal PPy overlayer thickness = 30 nm); and (e) PPy bulk powder.

for acceleration up to the hypervelocity regime when using a van de Graaff instrument.[17,27]

Zeta potential versus pH curves were determined for both the milled anthracene microparticles and the PPy-coated anthracene microparticles via aqueous electrophoresis (see Figure 9). The former microparticles exhibited negative zeta potentials (approximately −40 to −50 mV) regardless of the solution pH, which is consistent with the surface presence of the anionic Morwet D-425 dispersant. In contrast, the PPy-coated anthracene microparticles exhibited an isoelectric point at around pH 7.7 and acquired cationic character at low pH (e.g., −30 mV at pH 3). These observations are consistent with the deposition of an electrically conductive PPy overlayer at the surface of the anthracene microparticles.

The milled 4 μm anthracene microparticles prepared using the Morwet D-425 dispersant, PPy bulk powder, and a series of

https://dx.doi.org/10.1021/acsami.0c19758
ACS Appl. Mater. Interfaces 2021, 13, 3175−3185

PPy-coated anthracene microparticles were studied using XPS. In addition to the expected strong C1s signal, the survey spectrum recorded for the milled anthracene microparticles also contained Si2s and Si2p signals (Figure 10). These features are attributed to the silicone-based antifoam agent, which is not fully removed after the centrifugation−redispersion wash cycles. A weak S2p signal was also discernible, which is assigned to the anionic sulfonate groups of the Morwet D-425 dispersant (see Figure 1c). The survey spectra recorded for this commercial dispersant and the as-received (unmilled) anthracene crystals are provided in the Supporting Information (see Figure S5).

As expected, the survey spectrum obtained for PPy bulk powder contains both N1s and Cl2p signals.[58] These signals are also detected in the spectra recorded for the series of three PPy-coated anthracene microparticles (nominal PPy overlayer thicknesses = 10, 20 and 30 nm). Comparing the relative intensities of the O1s and N1s signals for each of these three spectra, it is clear that the latter signal becomes progressively stronger as thicker PPy overlayers are targeted. The Cl/N atomic ratio calculated for the PPy bulk powder spectrum is 0.23, which is consistent with the chloride-doped, electrically conductive form of this organic polymer.[58,59] Similar Cl/N atomic ratios (0.22−0.30) were determined for the PPy overlayers deposited at the surface of the anthracene microparticles. Moreover, the S2p and Si2s/Si2p signals assigned to the Morwet D-425 dispersant and the silicone defoamer, respectively, gradually become attenuated as higher mass PPy loadings are targeted. It is also noteworthy that the survey spectra recorded for the PPy bulk powder and the PPy-coated anthracene microparticles (nominal PPy overlayer thickness = 30 nm) are strikingly similar. Such observations are understandable given the highly surface-specific nature of XPS analysis, which has a typical sampling depth of not more than 10 nm.[60] Finally, C1s core-line spectra for selected samples are shown in Figure S6. Interestingly, the C1s core-line spectrum recorded for the uncoated anthracene microparticles is significantly shifted in its binding energy compared to those recorded for PPy alone and the three examples of PPy-coated anthracene microparticles. This provides good evidence that the former sample is electrically insulating, whereas the latter four samples are electrically conductive, as expected.[60]

A preliminary hypervelocity experiment was conducted using a two-stage light gas gun[27] to fire PPy-coated 4 μm anthracene microparticles (nominal PPy overlayer thickness = 30 nm) at 1.87 km s^{-1} into an aluminum foil target (mean foil thickness = 110 μm). Subsequent SEM studies of this target revealed impact craters created by the impinging microparticles (see Figures 11a and S7). These craters are relatively shallow, with barely raised lips at their edges. There is no visible sign of significant projectile fragments or residue lining the craters. Nevertheless, a faint ring of carbonaceous debris is discernible when the same crater is subjected to X-ray elemental mapping analysis (see Figures 11b and S7). Some larger carbon-rich fragments are also visible that may also originate from the impinging projectile. However, we cannot be certain that the latter debris does not originate from contamination by the sabot employed in this light gas gun experiment.

These observations can be compared to earlier attempts to simulate what would happen if organic microparticles entrained in the water plumes emitted from icy satellites of Jupiter and Saturn (i.e., Europa and Enceladus, respectively)

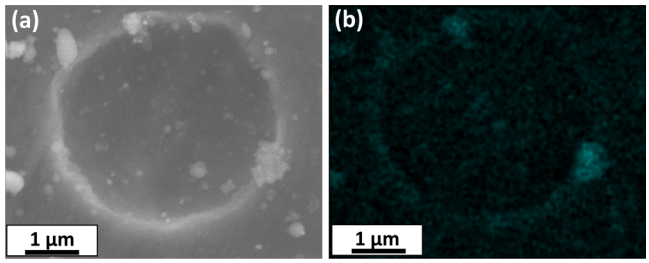

Figure 11. (a) SEM image of an impact crater formed by firing PPy-coated anthracene microparticles (4 μm diameter; coated with a nominal PPy overlayer thickness of 30 nm) at an aluminum foil target (mean thickness = 110 μm) at 1.87 km s^{-1} using a two-stage light gas gun. (b) Corresponding elemental carbon image obtained when using X-ray elemental mapping to examine the same impact crater. Carbonaceous debris is discernible as a faint crater ring, with some larger fragments also being visible (see main text for further details).

were to be intercepted by a passing spacecraft. For example, New et al.[61] fired poly(methyl methacrylate) microparticles of 4, 6, and 10 μm diameter at five different metal targets (including aluminum) at hypervelocities ranging from 0.5 to 3 km s^{-1}. Below the hypervelocity regime (<1 km s^{-1}), the impinging microparticles either adhered or rebounded. At hypervelocities of around 1 km s^{-1}, imprints were left in the surface of the metal target, with carbon residues being detected by X-ray elemental mapping analysis. At 2−3 km s^{-1}, craters lined with partially melted residues were obtained. Up to and including impacts at 2 km s^{-1}, Raman microscopy studies confirmed the presence of PMMA fragments, but at higher speeds, no such debris was found. This is consistent with the prior work by Burchell and co-workers,[33] who found that PPy-coated polystyrene microparticles of 20 μm diameter survived intact when fired at aerogel targets at up to 2 km s^{-1} but underwent extensive thermal ablation when impinging at higher hypervelocities. Separately, Burchell and Harriss[62] recently reported that firing polystyrene and PMMA microparticles at aluminum targets at 5 km s^{-1} produced impact craters that were solely lined with carbonaceous residues—there were no identifiable polystyrene or PMMA residues. The preliminary data reported herein extend the growing number of hypervelocity impact studies involving organic microparticles to include PAH-rich projectiles. Moreover, they suggest that the chemical nature of the projectile is an important factor, so the earlier observations made for PMMA microparticles cannot be assumed to be valid for all types of organic microparticles. Thus, given the ubiquity of PAH throughout the universe, it is clearly important to develop suitable synthetic mimics to understand the behavior of this type of organic cosmic dust.

CONCLUSIONS

The simplest member of the PAH family, anthracene, can be conveniently prepared in the form of microparticles by ball-milling macroscopic organic crystals using a commercial polymeric dispersant (Morwet D-425). These precursor microparticles were then coated with PPy, an air-stable electrically conductive polymer. Both the original uncoated microparticles and the PPy-coated microparticles were characterized by optical microscopy, laser diffraction, aqueous electrophoresis, SEM, vibrational spectroscopy, and XPS. These techniques are consistent with the presence of an ultrathin contiguous overlayer of PPy on the surface of the

https://dx.doi.org/10.1021/acsami.0c19758
ACS Appl. Mater. Interfaces 2021, 13, 3175−3185

anthracene microparticles. Such microparticles are expected to be useful synthetic mimics for PAH-rich cosmic dust, which is found throughout the universe. Finally, we demonstrate that a light gas gun[27,33,34] can be used to accelerate such microparticles up to the hypervelocity regime. Moreover, we note that the electrically conductive nature of the PPy overlayer should enable the efficient accumulation of surface charge[17,27,35] and hence provide access to higher hypervelocities using a van de Graaff accelerator. In such experiments, this overlayer is also likely to be a useful sacrificial layer for assessing the extent of thermal ablation of such microparticles during their capture within aerogel targets.[33]

■ ASSOCIATED CONTENT

Supporting Information

The Supporting Information is available free of charge at https://pubs.acs.org/doi/10.1021/acsami.0c19758.

Equation used to calculate PPy overlayer thickness assuming a core−shell spherical morphology; SEM images recorded for 2 μm anthracene microparticles before and after coating with a nominal 20 nm PPy overlayer; laser diffraction particle size distributions recorded for uncoated anthracene microparticles before and after removing excess Morwet D-425 via centrifugation; linear calibration plot for aqueous solution density of Morwet D-425 versus concentration to determine extent of adsorption of this dispersant on milled anthracene microparticles; SEM images recorded for PPy bulk powder; X-ray photoelectron spectra recorded for unmilled anthracene crystals, Morwet D-425 alone and 4 μm anthracene microparticles prepared using this commercial dispersant; X-ray photoelectron C1s core-line spectra recorded for uncoated 4 μm anthracene microparticles, PPy-coated 4 μm anthracene microparticles, and PPy bulk powder; and energy-dispersive X-ray spectrum recorded for an impact crater generated during a light gas gun experiment (PDF)

■ AUTHOR INFORMATION

Corresponding Author

Steven P. Armes − *Department of Chemistry, University of Sheffield, Sheffield, South Yorkshire S3 7HF, U.K.*; orcid.org/0000-0002-8289-6351; Email: S.P.Armes@sheffield.ac.uk

Authors

Derek H. Chan − *Department of Chemistry, University of Sheffield, Sheffield, South Yorkshire S3 7HF, U.K.*

Arthur Millet − *Department of Chemistry, University of Sheffield, Sheffield, South Yorkshire S3 7HF, U.K.*

Callum R. Fisher − *Centre for Astrophysics and Planetary Science, School of Physical Sciences, University of Kent, Canterbury, Kent CT2 7NH, U.K.*

Mark C. Price − *Centre for Astrophysics and Planetary Science, School of Physical Sciences, University of Kent, Canterbury, Kent CT2 7NH, U.K.*

Mark J. Burchell − *Centre for Astrophysics and Planetary Science, School of Physical Sciences, University of Kent, Canterbury, Kent CT2 7NH, U.K.*; orcid.org/0000-0002-2680-8943

Complete contact information is available at: https://pubs.acs.org/10.1021/acsami.0c19758

Notes

The authors declare no competing financial interest.

■ ACKNOWLEDGMENTS

S.P.A. acknowledges a four-year EPSRC *Established Career* Particle Technology Fellowship (EP/R003009). Syngenta are acknowledged for an EPSRC Industrial CASE studentship for D.H.C. and also for permission to publish this work. C.R.F. thanks STFC for a PhD studentship. STFC also funded use of the U. Kent Light Gas Gun via a Consolidated Grant.

■ REFERENCES

(1) Abdel-Shafy, H. I.; Mansour, M. S. M. A Review on Polycyclic Aromatic Hydrocarbons: Source, Environmental Impact, Effect on Human Health and Remediation. *Egypt. J. Pet.* **2016**, *25*, 107−123.

(2) Allamandola, L. J.; Sandford, S. A.; Wopenka, B. Interstellar Polycyclic Aromatic Hydrocarbons and Carbon in Interplantary Dust Particles and Meteorites. *Science* **1987**, *237*, 56−59.

(3) Allamandola, L. J.; Tielens, G. G. M.; Barker, J. R. Interstellar Polycyclic Aromatic Hydrocarbons: The Infrared Emission Bands, The Excitation/Emission Mechanism, and the Astrophysical Implications. *Astrophys. J., Suppl. Ser.* **1989**, *71*, 733−775.

(4) Tielens, A. G. G. M. Interstellar Polycyclic Aromatic Hydrocarbon Molecules. *Annu. Rev. Astron. Astrophys.* **2008**, *46*, 289−337.

(5) Roser, J. E.; Ricca, A. Polycyclic Aromatic Hydrocarbon Clusters as Sources of Interstellar Infrared Emission. *Astrophys. J.* **2015**, *801*, 108.

(6) Greenberg, J. M.; Gillette, J. S.; Muñoz Caro, G. M.; Mahajan, T. B.; Zare, R. N.; Li, A.; Schutte, W. A.; de Groot, M.; Mendoza-Gómez, C. Ultraviolet Photoprocessing of Interstellar Dust Mantles as a Source of Polycyclic Aromatic Hydrocarbons and Other Conjugated Molecules. *Astrophys. J.* **2000**, *531*, L71−L73.

(7) Steele, A.; Mccubbin, F. M.; Fries, M.; Kater, L.; Boctor, N. Z.; Fogel, M. L.; Conrad, P. G.; Glamoclija, M.; Spencer, M.; Morrow, A. L.; Hammond, M. R.; Zare, R. N.; Vicenzi, E. P.; Siljestrom, S.; Bowden, R.; Herd, C. D. K.; Mysen, B. O.; Shirey, S. B.; Amundsen, H. E. F.; Treiman, A. H.; Bullock, E. S.; Jull, A. J. T. A Reduced Organic Carbon Component in Martian Basalts. *Science* **2012**, *337*, 212−215.

(8) Derenne, S.; Robert, F. Model of Molecular Structure of the Insoluble Organic Matter Isolated from Murchison Meteorite. *Meteorit. Planet. Sci.* **2010**, *45*, 1461−1475.

(9) López-Puertas, M.; Dinelli, B. M.; Adriani, A.; Funke, B.; Moriconi, M. L.; Boersma, C.; Allamandola, L. J. Large Abundances Of Polycyclic Aromatic Hydrocarbons in Titan's Upper Atmosphere. *Astrophys. J.* **2013**, *770*, 1−8.

(10) Zhao, L.; Kaiser, R. I.; Xu, B.; Ablikim, U.; Ahmed, M.; Evseev, M. M.; Bashkirov, E. K.; Azyazov, V. N.; Mebel, A. M. Low-Temperature Formation of Polycyclic Aromatic Hydrocarbons in Titan's Atmosphere. *Nat. Astron.* **2018**, *2*, 973−979.

(11) Moreels, G.; Clairemidi, J.; Hermine, P.; Brechignac, P.; Rousselot, P. Detection of a Polycyclic Aromatic Molecule in Comet P/Halley. *Astron. Astrophys.* **1994**, *282*, 643−656.

(12) Clairemidi, J.; Bréchignac, P.; Moreels, G.; Pautet, D. Tentative Identification of Pyrene as a Polycyclic Aromatic Molecule in UV Spectra of Comet P/Halley: An Emission from 368 to 384 Nm. *Planet. Space Sci.* **2004**, *52*, 761−772.

(13) Clemett, S. J.; Maechling, C. R.; Zare, R. N.; Swan, P. D.; Walker, R. M. Identification of Complex Aromatic Molecules in Individual Interplanetary Dust Particles. *Science* **1993**, *262*, 721−725.

(14) Ehrenfreund, P.; Rasmussen, S.; Cleaves, J.; Chen, L. Experimentally Tracing the Key Steps in the Origin of Life: The Aromatic World. *Astrobiology* **2006**, *6*, 490−520.

(15) Stockton, A. M.; Chiesl, T. N.; Scherer, J. R.; Mathies, R. A. Polycyclic Aromatic Hydrocarbon Analysis with the Mars Organic

Analyzer Microchip Capillary Electrophoresis System. *Anal. Chem.* **2009**, *81*, 790−796.
(16) Fielding, L. A.; Hillier, J. K.; Burchell, M. J.; Armes, S. P. Space Science Applications for Conducting Polymer Particles: Synthetic Mimics for Cosmic Dust and Micrometeorites. *Chem. Commun.* **2015**, *51*, 16886−16899.
(17) Burchell, M. J.; Cole, M. J.; Lascelles, S. F.; Khan, M. A.; Barthet, C.; Wilson, S. A.; Cairns, D. B.; Armes, S. P. Acceleration of Conducting Polymer-Coated Latex Particles as Projectiles in Hypervelocity Impact Experiments. *J. Phys. D: Appl. Phys.* **1999**, *32*, 1719−1728.
(18) Srama, R.; Woiwode, W.; Postberg, F.; Armes, S. P.; Fujii, S.; Dupin, D.; Ormond-Prout, J.; Sternovsky, Z.; Kempf, S.; Moragas-Klostermeyer, G.; Mocker, A.; Grün, E. Mass Spectrometry of Hyper-Velocity Impacts of Organic Micrograins. *Rapid Commun. Mass Spectrom.* **2009**, *23*, 3895−3906.
(19) Mellado, E. M.; Hornung, K.; Srama, R.; Kissel, J.; Armes, S. P.; Fujii, S. Mass Spectrometry of Impact Fragmented Polymers: The Role of Target Properties. *Int. J. Impact Eng.* **2011**, *38*, 486−494.
(20) Goldsworthy, B. J.; Burchell, M. J.; Cole, M. J.; Armes, S. P.; Khan, M. A.; Lascelles, S. F.; Green, S. F.; McDonnell, J. A. M.; Srama, R.; Bigger, S. W. Time of Flight Mass Spectra of Ions in Plasmas Produced by Hypervelocity Impacts of Organic and Mineralogical Microparticles on a Cosmic Dust Analyser. *Astron. Astrophys.* **2003**, *409*, 1151−1167.
(21) Goldsworthy, B. J.; Burchell, M. J.; Cole, M. J.; Green, S. F.; Leese, M. R.; McBride, N.; McDonnell, J. A. M.; Müller, M.; Grün, E.; Srama, R.; Armes, S. P.; Khan, M. A. Laboratory Calibration of the Cassini Cosmic Dust Analyser (CDA) Using New, Low Density Projectiles. *Adv. Space Res.* **2002**, *29*, 1139−1144.
(22) Srama, R.; Ahrens, T. J.; Altobelli, N.; Auer, S.; Bradley, J. G.; Burton, M.; Dikarev, V. V.; Economou, T.; Fechtig, H.; Görlich, M.; Grande, M.; Graps, A.; Grün, E.; Havnes, O.; Helfert, S.; Horanyi, M.; Igenbergs, E.; Jessberger, E. K.; Johnson, T. V.; Kempf, S.; Krivov, A. V.; Krüger, H.; Mocker-Ahlreep, A.; Moragas-Klostermeyer, G.; Lamy, P.; Landgraf, M.; Linkert, D.; Linkert, G.; Lura, F.; McDonnell, J. A. M.; Möhlmann, D.; Morfill, G. E.; Müller, M.; Roy, M.; Schäfer, G.; Schlotzhauer, G.; Schwehm, G. H.; Spahn, F.; Stübig, M.; Svestka, J.; Tschernjawski, V.; Tuzzolino, A. J.; Wäsch, R.; Zook, H. A. The Cassini Cosmic Dust Analyzer. *Space Sci. Rev.* **2004**, *114*, 465−518.
(23) Postberg, F.; Khawaja, N.; Abel, B.; Choblet, G.; Glein, C. R.; Gudipati, M. S.; Henderson, B. L.; Hsu, H.-W.; Kempf, S.; Klenner, F.; Moragas-Klostermeyer, G.; Magee, B.; Nölle, L.; Perry, M.; Reviol, R.; Schmidt, J.; Srama, R.; Stolz, F.; Tobie, G.; Trieloff, M.; Waite, J. H. Macromolecular Organic Compounds from the Depths of Enceladus. *Nature* **2018**, *558*, 564−568.
(24) Khawaja, N.; Postberg, F.; Hillier, J.; Klenner, F.; Kempf, S.; Nölle, L.; Reviol, R.; Zou, Z.; Srama, R. Low-Mass Nitrogen-, Oxygen-Bearing, and Aromatic Compounds in Enceladean Ice Grains. *Mon. Not. R. Astron. Soc.* **2019**, *489*, 5231−5243.
(25) Lascelles, S. F.; Armes, S. P. Synthesis and Characterization of Micrometre-Sized , Polypyrrole-Coated Polystyrene Latexes. *J. Mater. Chem.* **1997**, *7*, 1339−1347.
(26) Lovett, J. R.; Fielding, L. A.; Armes, S. P.; Buxton, R. One-Pot Preparation of Conducting Polymer-Coated Silica Particles: Model Highly Absorbing Aerosols. *Adv. Funct. Mater.* **2014**, *24*, 1290−1299.
(27) Burchell, M. J.; Cole, M. J.; McDonnell, J. A. M.; Zarnecki, J. C. Hypervelocity Impact Studies Using the 2 MV Van de Graaff Accelerator and Two-Stage Light Gas Gun of the University of Kent at Canterbury. *Meas. Sci. Technol.* **1999**, *10*, 41−50.
(28) Li, Y. W.; Bugiel, S.; Trieloff, M.; Hillier, J. K.; Postberg, F.; Price, M. C.; Shu, A.; Fiege, K.; Fielding, L. A.; Armes, S. P.; Wu, Y. Y.; Grün, E.; Srama, R. Morphology of Craters Generated by Hypervelocity Impacts of Micron-Sized Polypyrrole-Coated Olivine Particles. *Meteorit. Planet. Sci.* **2014**, *49*, 1375−1387.
(29) Hillier, J. K.; Sternovsky, Z.; Armes, S. P.; Fielding, L. A.; Postberg, F.; Bugiel, S.; Drake, K.; Srama, R.; Kearsley, A. T.; Trieloff, M. Impact Ionisation Mass Spectrometry of Polypyrrole-Coated Pyrrhotite Microparticles. *Planet. Space Sci.* **2014**, *97*, 9−22.
(30) Postberg, F.; Hillier, J. K.; Armes, S. P.; Bugiel, S.; Butterworth, A.; Dupin, D.; et al. Stardust Interstellar Preliminary Examination IX: High-Speed Interstellar Dust Analog Capture in Stardust Flight-Spare Aerogel. *Meteorit. Planet. Sci.* **2014**, *49*, 1666−1679.
(31) One reviewer has requested that we mention that alternative conductive overlayers can be deposited. For example, putative projectiles can be coated with precious metals such as platinum but this usually leads to the deposition of relatively thick dense overlayers (see Hillier, J. K.; Sestak, S.; Green, S. F.; Postberg, F.; Srama, R.; Trieloff, M. The Production of Platinum-Coated Silicate Nanoparticle Aggregates for Use in Hypervelocity Impact Experiments. *Planet. Space Sci.* **2009**, *57*, 2081−2086.
(32) Burchell, M. J.; Armes, S. P. Impact Ionisation Spectra from Hypervelocity Impacts Using Aliphatic Poly(Methyl Methacrylate) Microparticle Projectiles. *Rapid Commun. Mass Spectrom.* **2011**, *25*, 543−550.
(33) Burchell, M. J.; Foster, N. J.; Ormond-Prout, J.; Dupin, D.; Armes, S. P. Extent of Thermal Ablation Suffered by Model Organic Microparticles during Aerogel Capture at Hypervelocities. *Meteorit. Planet. Sci.* **2009**, *44*, 1407−1419.
(34) Wozniakiewicz, P. J.; Price, M. C.; Armes, S. P.; Burchell, M. J.; Cole, M. J.; Fielding, L. A.; Hillier, J. K.; Lovett, J. R. Micron-Scale Hypervelocity Impact Craters: Dependence of Crater Ellipticity and Rim Morphology on Impact Trajectory, Projectile Size, Velocity, and Shape. *Meteorit. Planet. Sci.* **2014**, *49*, 1929−1947.
(35) Burchell, M. J.; Willis, M. J.; Armes, S. P.; Khan, M. A.; Percy, M. J.; Perruchot, C. Impact Ionization Experiments with Low Density Conducting Polymer-Based Micro-Projectiles as Analogues of Solar System Dusts. *Planet. Space Sci.* **2002**, *50*, 1025−1035.
(36) Cloutis, E.; Szymanski, P.; Applin, D.; Goltz, D. Identification and Discrimination of Polycyclic Aromatic Hydrocarbons Using Raman Spectroscopy. *Icarus* **2016**, *274*, 211−230.
(37) Ormond-Prout, J.; Dupin, D.; Armes, S. P.; Foster, N. J.; Burchell, M. J. Synthesis and Characterization of Polypyrrole-Coated Poly(Methyl Methacrylate) Latex Particles. *J. Mater. Chem.* **2009**, *19*, 1433−1442.
(38) Haas, S.; Hässlin, H.-W.; Schlatter, C. Influence of Polymeric Surfactants on Pesticidal Suspension Concentrates: Dispersing Ability, Milling Efficiency and Stabilization Power. *Colloid. Surface. Physicochem. Eng. Aspect.* **2001**, *183−185*, 785−793.
(39) Stern, A. J.; Elsik, C. M. New Polymeric Comb Dispersants for Agricultural Formulations: A Comparison of Performance in Pesticide Suspension Concentrates. *J. ASTM Int.* **2007**, *4*, 34−42.
(40) Narayanan, K. S.; Jon, D. I.; Patel, J. New Value-Added Polymeric Dispersants and Uses Thereof in Agricultural Formulations. *J. ASTM Int.* **2005**, *2*, 299−312.
(41) Bell, G. A. *Chemistry and Technology of Agrochemical Formulations*; Knowles, A., Ed.; Springer Dordrecht, 1998.
(42) Hörz, F.; et al. Impact Features on Stardust: Implications for Comet 81P/Wild 2 Dust. *Science* **2006**, *314*, 1716−1719.
(43) Burchell, M. J.; Fairey, S. A. J.; Wozniakiewicz, P.; Brownlee, D. E.; Hörz, F.; Kearsley, A. T.; See, T. H.; Tsou, P.; Westphal, A.; Green, S. F.; Trigo-Rodríguez, J. M.; Domingúez, G. Characteristics of Cometary Dust Tracks in Stardust Aerogel and Laboratory Calibrations. *Meteorit. Planet. Sci.* **2008**, *43*, 23−40.
(44) Lorenz, R. D. Europa Ocean Sampling by Plume Flythrough: Astrobiological Expectations. *Icarus* **2016**, *267*, 217−219.
(45) Guzman, M.; Lorenz, R.; Hurley, D.; Farrell, W.; Spencer, J.; Hansen, C.; Hurford, T.; Ibea, J.; Carlson, P.; McKay, C. P. Collecting Amino Acids in the Enceladus Plume. *Int. J. Astrobiol.* **2019**, *18*, 47−59.
(46) Fujii, S.; Armes, S. P.; Jeans, R.; Devonshire, R.; Warren, S.; McArthur, S. L.; Burchell, M. J.; Postberg, F.; Srama, R. Synthesis and Characterization of Polypyrrole-Coated Sulfur-Rich Latex Particles: New Synthetic Mimics for Sulfur-Based Micrometeorites. *Chem. Mater.* **2006**, *18*, 2758−2765.
(47) Maeda, S.; Armes, S. P. Preparation and Characterization of Novel Polypyrrole-Silica Colloidal Nanocomposites. *J. Mater. Chem.* **1994**, *4*, 935−942.

https://dx.doi.org/10.1021/acsami.0c19758
ACS Appl. Mater. Interfaces 2021, 13, 3175−3185

(48) Han, M. G.; Armes, S. P. Preparation and Characterization of Polypyrrole-Silica Colloidal Nanocomposites in Water-Methanol Mixtures. *J. Colloid Interface Sci.* **2003**, *262*, 418−427.
(49) Lo, M.; Pires, R.; Diaw, K.; Gningue-Sall, D.; Oturan, M. A.; Aaron, J.-J.; Chehimi, M. M. Diazonium Salts: Versatile Molecular Glues for Sticking Conductive Polymers to Flexible Electrodes. *Surfaces* **2018**, *1*, 43−58.
(50) Cawdery, N.; Obey, T. M.; Vincent, B. Colloidal Dispersions of Electrically Conducting Polypyrrole Particles in Various Media. *J. Chem. Soc., Chem. Commun.* **1988**, 1189−1190.
(51) Armes, S. P.; Aldissi, M.; Hawley, M.; Beery, J. G.; Gottesfeld, S. Morphology and Structure of Conducting Polymers. *Langmuir* **1991**, *7*, 1447−1452.
(52) Räsänen, J.; Stenman, F.; Penttinen, E. Raman Scattering from Molecular Crystals–II . Anthracene. *Spectrochim. Acta, Part A* **1973**, *29*, 395−403.
(53) Cheung, K. M.; Smith, B. J. E.; Batchelder, D. N.; Bloor, D. Raman Spectroscopy of Conductive Polypyrroles. *Synth. Met.* **1987**, *21*, 249−253.
(54) Furukawa, Y.; Tazawa, S.; Fujii, Y.; Harada, I. Raman Spectra of Polypyrrole and Its 2,5-13C-Substituted and C-Deuterated Analogues in Doped and Undoped States. *Synth. Met.* **1988**, *24*, 329−341.
(55) Liu, Y.-C. Characteristics of Vibration Modes of Polypyrrole on Surface-Enhanced Raman Scattering Spectra. *J. Electroanal. Chem.* **2004**, *571*, 255−264.
(56) Tooru, I.; Ikuo, H.; Toshihiro, Y. Change of Raman Scattering Intensity of a Polypyrrole Film during Reversible Doping and Emitting Processes of ClO_4^-. *Chem. Lett.* **1987**, *16*, 563−566.
(57) Lascelles, S. F.; Armes, S. P.; Zhdan, P. A.; Greaves, S. J.; Brown, A. M.; Watts, J. F.; Leadley, S. R.; Luk, S. Y. Surface Characterization of Micrometre-Sized, Polypyrrole-Coated Polystyrene Latexes: Verification of a "core-Shell" Morphology. *J. Mater. Chem.* **1997**, *7*, 1349−1355.
(58) Perruchot, C.; Chehimi, M. M.; Delamar, M.; Lascelles, S. F.; Armes, S. P. Surface Characterization of Polypyrrole-Coated Polystyrene Latex by X-Ray Photoelectron Spectroscopy. *Langmuir* **1996**, *12*, 3245−3251.
(59) Armes, S. P. Optimum Reaction Conditions for the Polymerization of Pyrrole by Iron(III) Chloride in Aqueous Solution. *Synth. Met.* **1987**, *20*, 365−371.
(60) Watts, J. F., Wolstenholme, J. *An Introduction to Surface Analysis by XPS and AES*; Wiley Chichester, 2003.
(61) New, J. S.; Mathies, R. A.; Price, M. C.; Cole, M. J.; Golozar, M.; Spathis, V.; Burchell, M. J.; Butterworth, A. L. Characterizing Organic Particle Impacts on Inert Metal Surfaces: Foundations for Capturing Organic Molecules during Hypervelocity Transits of Enceladus Plumes. *Meteorit. Planet. Sci.* **2020**, *55*, 465−479.
(62) Burchell, M.; Harriss, K. Organic Molecules: Is It Possible to Distinguish Aromatics from Aliphatics Collected by Space Missions in High Speed Impacts? *Sci* **2020**, *2*, 56.

https://dx.doi.org/10.1021/acsami.0c19758
ACS Appl. Mater. Interfaces 2021, 13, 3175−3185